
Article:
Dove, C.A., Bradley, F.F. and Patwardhan, S.V. orcid.org/0000-0002-4958-8840 (2019) A material characterization and embodied energy study of novel clay-alginate composite aerogels. Energy and Buildings, 184. pp. 88-98. ISSN 0378-7788

https://doi.org/10.1016/j.enbuild.2018.10.045

Clay-Alginate Composite Aerogels as Insulation Materials

Cassandra A. Dove [a], Fiona F. Bradley [b]*, Siddharth V. Patwardhan [c]

[a] Dept. of Architecture, University of Strathclyde, Glasgow, UK
[b] School of Engineering, University of Glasgow, Glasgow, UK
[c] Department of Chemical and Biological Engineering, University of Sheffield, UK

ABSTRACT

There is a growing incentive within the construction industry to design low energy buildings which incorporate increased levels of insulation whilst also encouraging the use of 'green' materials which have a low environmental impact and can contribute positively to sustainable building strategies. Silica aerogels have received an increasing amount of attention in recent years as a contemporary insulation material, but their wide-spread use is currently hindered by high costs and their high embodied energy. This research project explores the development of a composite insulation material proposed as an alternative to silica aerogel, which consists of natural components including clay and a biopolymer obtained from seaweed known as alginate. Prototype specimens have been developed and characterised in terms of their mechanical properties and microstructure allowing comparisons to be made between five alginate types, each obtained from a different seaweed source. Whilst all of the composites tested offered an improvement over the control sample, the results also demonstrated that the type of alginate used has a significant influence on the compressive strength and modulus values of the resulting composite materials. An analysis of the production process additionally demonstrated that the freeze-drying element can have a significant impact on both the environment and financial costs of producing such a material.

Keywords: biopolymer; biocomposite; alginate; aerogel; clay; insulation

1. INTRODUCTION

Since two thirds of the heat generated in a building can be lost through the building fabric (Carbon Trust, 2012), the use of appropriate thermal insulation is critical in helping to minimise energy losses and reduce fuel costs for the occupants. It also decreases the reliance on mechanical heating systems. Effective insulation materials are generally those which have a cellular or porous structure, a low density and a low thermal conductivity. Common products therefore include the likes of mineral wool which typically achieves a thermal conductivity of 0.3 – 0.4 W/m-K (Cuce et al., 2014a). Polymer based products such as polyurethane (PUR) and expanded polystyrene (EPS) are also particularly good insulators, exhibiting thermal conductivities as low as 0.2 – 0.3 W/m-K (Jelle, 2011). However these petrochemical derived insulation materials also exhibit poor environmental credentials due to energy-intensive processing techniques and the use of fluorocarbon gases (Papadopoulos, 2005). Furthermore, PUR based products also perform poorly in fire scenarios and can emit toxic substances such as hydrogen cyanide (Stec and Hull, 2011).

The use of natural, renewable materials has therefore been identified as a potential means of reducing the embodied energy and carbon footprint of buildings (Felton et al., 2013). Natural insulation products which include organic fibres such as those obtained from plant or animal sources have been commercialized in recent years and continue to be investigated with academic research (Korjenic et al., 2011; Lopez Hurtado et al., 2016; Zach et al., 2016; Pedroso et al., 2017; Savio et al., 2018). The thermal properties of these materials are often inferior to polymer based products meaning that greater thicknesses are required in order to achieve comparable performance. As discussed by Sutton et al. (2011) and Schiavoni et al. (2016), examples include wood fibre (0.038 to 0.050 W/mK), hemp (0.038 and 0.060 W/mK), sheep's wool (0.038 and 0.054 W/mK), flax (0.038 and 0.075 W/mK) and cork (0.038 and 0.075 W/mK). Natural materials are also disadvantaged in terms of their durability, moisture sensitivity and cost and therefore form only a small part of the UK market (Sutton et al., 2011). On the other hand, LCA studies (Schiavoni et al., 2016) have shown that the embodied energy and global warming potential values of natural fibre products are generally lower than polymer based products, although some natural products like cork can in fact be worse than the likes of EPS and PUR. Mineral wool products also perform well in LCA terms despite being produced from non-renewable resources. As a result, when selecting appropriate insulation materials, there is often a

trade-off made between technical performance, cost and environmental impact. Whilst mineral wool products remain the most popular choice for standard building insulation (Kiss et al., 2013), offering the best balance between cost and technical performance, alternatives which offer lower thermal conductivities are now being investigated for high-performance applications. One such development is the introduction of aerogels to the building insulation market. These materials originated from early research by Kistler (1932; 1934) and are prepared by removing the liquid phase from a hydrated gel using supercritical drying. The result is a highly porous, low density material which can be formed into an aerogel monoliths and granules or combined with another material to form a composite product (Nosrati and Berardi, 2018). The majority of commercially available aerogels are silica-based aerogels and these can be used as high performance insulation products for buildings in the form of boards, blankets or loose-fill granules (Jelle, 2011; Baetens et al., 2011;Thapliyal and Singh, 2014;Cuce et al., 2014a). They can also be incorporated into vacuum insulation panels (VIPs), a composite product consisting of a cellular core which is then vacuum sealed within a layer of foil faced plastic (Alam et al., 2011)(Liang et al., 2017b). More recent developments included insulated plasters which incorporate silica aerogels (Stahl et al., 2012; Buratti et al., 2017) and aerogel/glass fibre composites (Ul Haq et al., 2017). Aerogel products offer very low thermal conductivities for relatively small thicknesses, making them particularly useful within retrofit projects where space is often restricted (Martinez, 2017). High performance VIPs with an aerogel core can reportedly achieve thermal conductivities as low as 0.012 W/mK (Liang et al., 2017a) whilst (Buratti et al., 2017) describe aerogel granules with a thermal conductivity of 0.019–0.023 W/(mK). Commercial silica aerogel blankets also offer values of 0.018 W/mK (Aspen Aerogels, 2011). Silica-based aerogels are however disadvantaged with respect to their environmental performance due to the energy-intensive production processes and hazardous solvents used in their production (Dowson et al., 2012). In addition, high production costs are a limiting factor on their widespread use (Riffat and Qiu, 2013; Cuce et al., 2014a), particularly in the case of monolithic aerogels which have been more difficult to commercialize than granules an composite products (Nosrati and Berardi, 2018). Some authors have therefore proposed alternatives to silica based aerogels which are derived from more environmentally friendly precursors. Kistler (1932) for example experimented with various natural substances such as cellulose, gelatine and agar during his early work and van Olphen (1967) also studied various water-soluble polymers in combination with clay minerals. Aerogels produced from other natural polymers such as starch (Druel

et al., 2017) are also being investigated as a means of producing thermal insulation materials. More recently, Schiraldi, Bandi & Gawryla (2006) have developed a product known as Aeroclay™ using clay aerogels modified by a range of polymeric sustances: epoxy (Arndt et al., 2007); PVOH and various natural fibres (Finlay et al., 2007; Chen et al., 2014); casein (Gawryla et al., 2008), natural rubber (Pojanavaraphan et al., 2010a) and alginate (Chen et al., 2012). Reportedly, these clay-based composites can be manufactured at a competitive price utilising a relatively simple freeze-drying process, making them potential alternatives to silica aerogels (Dalton et al., 2010; Schiraldi et al., 2010). As discussed by (Madyan et al., 2016), the physical properties of clay aerogels, including the density, thermal conductivity and combustion behavior, can also be tailored by modifying the processing conditions and through the use of various additives or coatings. There are however limited details of the embodied energy of clay aerogels and to what extent the inclusion of additives, whether synthetic or bio-based, influences their overall environmental impact.

Given that the ideal product would be one which offers thermal properties comparable to high performance insulations combined with minimal environmental impacts it was postulated that a clay-polymer aerogel consisting of natural raw materials may offer a potential solution. For the purposes of this study, a natural bentonite clay and one of the aforementioned biopolymers, alginate, were used to create a series of composite aerogel materials which could be studied in relation to both their physical properties and production. Whilst a few studies have demonstrated that aerogels with high porosity and low bulk density can be created using layered silicates and alginate (Ohta and Nakazawa, 1995; Chen et al., 2012), the role of the alginate, which is a biopolymer obtained from seaweed, is not discussed in great detail. This is an important aspect to consider given that alginate is a natural material which can vary widely in its composition and functionality depending of the specific seaweed from which it is sourced. There has therefore been no comprehensive study to date which discusses the role of alginate variables (source, M/G ratio, viscosity and concentration) on the structural properties of composite alginate-clay aerogels such as density, mechanical strength and morphology. A total of five different alginate products were therefore tested in order to assess the feasibility of producing such a composite and to determine the relative importance of different alginate variables on the final properties of the aerogel. The final objective was to assess both the commercial viability and environmental impacts of the alginate-clay composite in comparison with other aerogel materials.

2. EXPERIMENTAL

2.1. Materials

2.1.1. Alginate

Alginate is a biopolymer obtained from brown seaweeds. More specifically, alginate is the collective term for the salts of alginic acid which are obtained from the cell walls of the macro-algae. These salts, usually in the form of sodium or potassium, contribute to 20-60% of the dry matter of the algae (Rehm, 2009). Alginate is obtained by firstly washing the milled seaweed in acid in order to eradicate the cross-linking ions and solubilize the alginate salts (McHugh, 2003). The resulting mixture is then filtered to separate the solid cell wall debris and cellulose residue from the alginate solution. The aquous sodium alginate is then dried and pulverised to produce a sodium alginate powder. As a block co-polymer of (1-4)-linked β-D-mannuronic acid and α-L-guluronic acid residues, alginate is often described in terms of its M/G ratio, relating to the proportions of the M (mannuronic) and G (guluronic) units on the polymer chain. One of the most useful functional properties of alginate is its gel-forming ability, particularly in the presence of multivalent cations such as Ca^{2+} (Draget et al., 2006; Funami et al., 2009). Variables which are known to effect the gelation mechanisms include the seaweed source, the molecular weight and the composition of the polymer (Martinsen et al., 1989; Straatmann and Borchard, 2003). The ratio of the crosslinking ions (e.g. Ca^{2+}) to the carboxyl groups present on the alginate has also been shown to influence the gelation behavior (Liu et al., 2003).

In this study 4 different alginate products were supplied by Marine Biopolymers Ltd. (Ayr, Scotland) and obtained from seaweeds harvested from the west coast of Scotland. These were prototype products which are currently under development and have not yet been commercialized. Two different seaweed types were studied: the Ascophyllum nodosum (PR52) and the Laminaria hyperborean, the latter of which was separated into the stem (PR22 and PR24) and frond (PR32) components to provide additional compositional variables. A commercial alginate (AC) from Acros Organics was also used for comparison. The properties of all five alginate types used are summarised in TABLE 1. M/G ratios were provided by MBL and calculated using ^{1}H-NMR spectroscopy following existing methods (Grasdalen et al., 1979; Davis et al., 2003). Viscosity measurements were conducted using a Brookfield R/S Rheometer using 1 w/v% alginate solutions in 0.1 M NaCl at a temperature of 25℃.

TABLE 1: Alginate Properties

Specimen	Source	M/G Ratio	Intrinsic Viscosity (L/g)
AC	Commercial Alginate	0.83	0.63
PR22	L. hyperborea (stem*)	1.04	0.26
PR24	L. hyperborea (stem*)	0.23	0.48
PR32	L. hyperborea (frond**)	0.72	0.2
PR52	Ascophyllum Nodosum	0.77	0.2

*Stem = stalk-like component which forms structural backbone
**Frond = leaf-like components attached to stem

2.1.2. Clay

The clay used was a bentonite clay sourced from Acros Organics (Geel, Belgium). The pH of the clay was measured using a 1:5 volume ratio of dry clay to a 0.01 mol/L $CaCl_2$ solution (BS EN 15933:2012). The liquid limit was calculated using the cone penetrometer method (BS 1377-2:1990) whilst the electrical conductivity was measured using a handheld conductivity meter. Cation exchange capacity and specific surface area were calculated from the Methylene Blue test (BS EN 933-9:2009) and the available calcium content was obtained by inductively coupled plasma (ICP) on a deionised water (DI) extract. The bentonite properties are summarised in TABLE 2.

TABLE 2: Bentonite Properties

pH	Liquid Limit (%)	Clay Mineralogy	Electrical Conductivity (µS/cm)	Cation Exchange Capacity (meq/100g)	Specific Surface Area (m^2/g)	Exchangeable Calcium (ppm)
8.6	76.7	Major: Montmorillonite, Quartz, Feldspar	1943	65	26	4,228

2.2. Specimen preparation

The clay-alginate aerogels in this study were prepared using methods similar to that of Schiraldi et al. (2010) whereby separate 10 wt% solutions of the alginate and clay were prepared in DI water. These were then mixed at a range of alg:clay ratios (A = 100:0, B = 75:25, C = 50:50, D = 25:75 and E = 0:100) and filled into in 2mL cryogenic vials. Flash freezing was conducted using iso-pentane and liquid nitrogen followed by a minimum of 24 hours drying in a Scanvac CoolSafe 110-4 PRO 4lt freeze dryer. The specimens were then removed from the dryer and stored in sealed vials until further testing. The samples produced were cylinders of approximately 9mm diameter.

2.3. Characterisation

General observations were made regarding the quality and homogeneity of the final specimens. Each aerogel monolith was also weighed and its dimensions measured using digital calipers. The unit mass (g) and unit volume (cm^3) were then used to calculate the bulk density (ρ). The mechanical strength of the specimens was investigated based on the procedures outlined in BS EN 826:2013 and as described in other similar studies (Nussinovitch et al., 1993; Chen et al., 2012; Martins et al., 2015). Although compressive strength is not the most important property for insulating materials since these materials are not typically load-bearing, they still require sufficient mechanical integrity to be handled. Comparing the strength characteristics of the different compositions also gives an indication of which combinations of the clay and alginate are most effective. Testing was conducted on the cylindrical specimens which were cut using a scalpel to a height of ~15mm. The surfaces of the two parallel faces were also gently sanded to create smooth surfaces. An INSTRON 5969 universal testing machine was then used to apply a compressive force (F) to the material using a displacement rate of 5 mm/min. The compressive strength (σ_m) of the specimens was then calculated from the initial cross-sectional area of the specimen (A_o) and the maximum force (F_m) at the yield point. Results were then calculated as the mean value of three test samples calculated to the nearest 0.1 N/mm^2.

$$\sigma_m = F_m / A_o \quad (1)$$

Compressive strain (ε) was calculated by dividing the change in specimen height (ΔH) by the original height ($H_{O)}$. The compression modulus of elasticity (E) was also calculated from the initial linear gradient of the stress-stain plot, prior to the yield point.

Since the size, shape and volume of the pores have an important influence on the mechanical strength, as well as transport properties such as and thermal conductivity and vapour permeability, the internal morphology of the samples was also investigated. SEM analysis was initially performed using a Field Emission (FE) microscope (HITACHI SU-6600) in order to generate magnified images of the microstructure of the aerogel specimens. Thin sections of the material were cut from the monoliths in order to expose the internal part of the aerogel and all samples were sputter coated in gold prior to the analysis. Further investigation of the microstructure was also achieved by comparing the porosities of the different samples. Common porosity measurement techniques such as Mercury

Intrusion Porisimetry (MIP) and N_2 adsorption are problematic for compressible materials since the pressures exerted during measurement can transform the structure thereby leading to false pore sizes (Scherer, 1998). In this case porosity was therefore estimated by calculating the theoretical porosity of each sample using Equation 4, using the methods of Rassis et al. (2003), Longo et al. (2013) and Wang et al. (2014), where ρ_b is the bulk density of the sample and ρ_p is the overall particle density. The latter value is calculated based on the mass fraction of each component and particle density estimates of 2.5 g/cm^3 for bentonite (Kogel et al., 2006) and 1.59 for alginate (Aspinall, 2014).

$$P = (1 - \frac{\rho_b}{\rho_p}) \text{ x } 100\% \quad \textbf{(2)}$$

2.4. Cost and Environmental Impacts

In considering the commercial feasibility of using an alginate-clay aerogel as a building insulation material, aspects such as cost and environmental impact were also investigated. Cost calculations were performed based on data supplied by MBL but it should be noted that the costs were based on lab-scale prototypes with a production volume of approximately 100 cm^3. The calculations were also based purely on the basic cost of consumables and the key production processes. Costs associated with equipment, labour and overheads have not been included at this stage. Although advanced LCA can be used to provide a detailed environmental profile for the whole-life cycle of a product, this would involve more extensive calculations and require data not yet available at this prototype stage. As a result only estimations of embodied energy and embodied CO_2 were considered based on the quantities of materials used and the energy consumed during the main production processes.

3. RESULTS AND DISCUSSION

3.1. General properties

In general the quality and homogeneity of the samples was found to improve upon the addition of alginate. Indeed the clay only samples (E) were very friable and crumbled into a powder upon removal from the vial meaning that suitable monoliths for further tests could not be produced. The alginate containing samples were much more stable and easier to handle although in some cases (AC-A, AC-D, PR24-A and PR24-B) visible air voids and defects were observed (FIGURE 1). These

defects appear to be the result of air-bubbles which are formed during the mixing process in the higher viscosity samples. This is similar to observations made by Gawryla et al. where high polymer contents and high viscosity mixtures were also found to lead to air entrapment (Gawryla et al., 2008).

FIGURE 1: Sample Images (PR24)

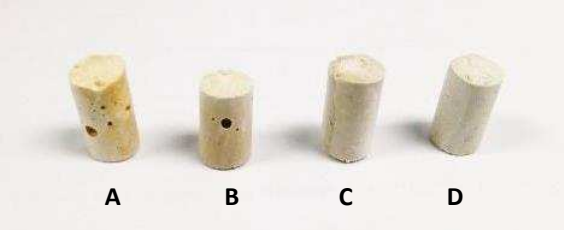

The bulk density values for all of the samples were found to be within 0.09 – 0.14 g/cm^3 range as shown in TABLE 3. This is within the range of medium density rigid polymer foams (0.08-0.17 g/m^3) (Ashby et al., 2013) but slightly higher than results from Chen et al. (2012) who report densities of 0.085 g/cm^3 for a clay-alginate aerogel with a mix ratio equivalent to the C samples in this study. The high variability in density, particularly for AC-A, is most likely due to the aforementioned presence of air voids within the specimens.

TABLE 3: Bulk Density (g/cm^3)

Alg:Clay	A (100:0)	B (75:25)	C (50:50)	D (25:75)
AC	0.12 (±0.03)	0.10 (±0.01)	0.12 (±0.01)	0.10 (±0.01)
PR22	0.13 (±0.02)	0.12 (±0.01)	0.10 (±0.01)	0.09 (±0.01)
PR24	0.10 (±0.01)	0.11 (±0.01)	0.11 (±0.01)	0.11 (±0.01)
PR32	0.11 (±0.01)	0.13 (±0.01)	0.09 (±0.03)	0.11 (±0.01)
PR52	0.11 (±0.01)	0.14 (±0.01)	0.11 (±0.01)	0.09(±0.02)

3.2. Mechanical Properties

3.2.1. Compressive Strength at Yield

Typical stress-strain plots for the aerogels are shown in FIGURE 2 to FIGURE 6, highlighting the variation between specimens incorporating different types of alginate. Most of the samples resulted in a similar profile with an initial linear portion followed by a visible yield point after and a sustained

period of elastic strain. In all cases the end of the initial linear phase occurred at low levels of strain which is similar to observations by Nussinovitch et al. (1993).

FIGURE 2: Stress-strain plots (AC)

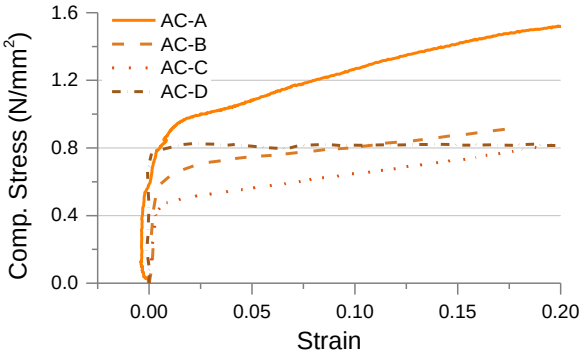

FIGURE 3: Stress-strain plots (PR22)

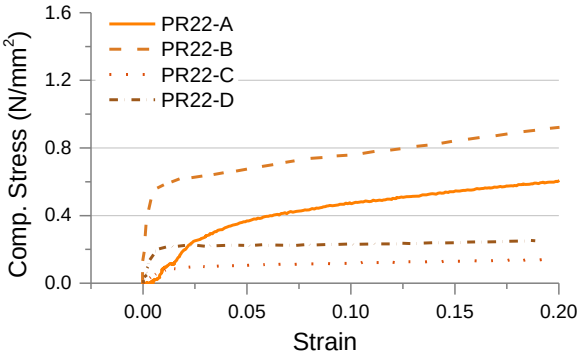

FIGURE 4: Stress-strain plots (PR24)

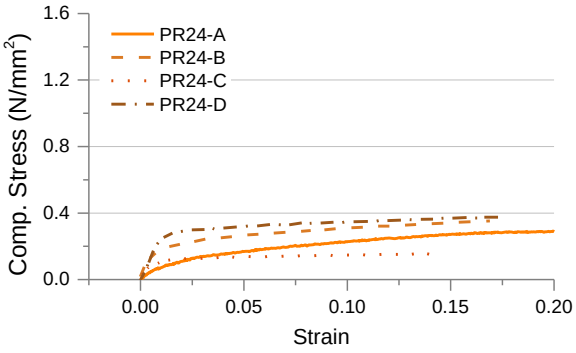

FIGURE 5: Stress-strain plots (PR32)

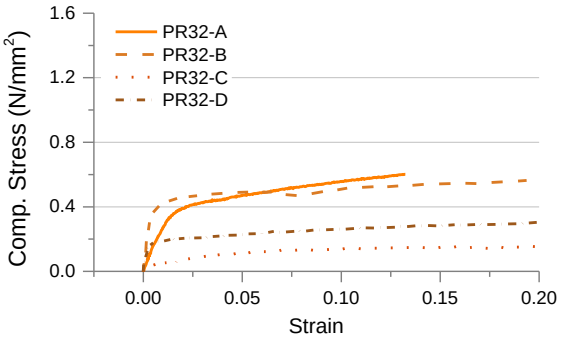

FIGURE 6: Stress-strain plots (PR52)

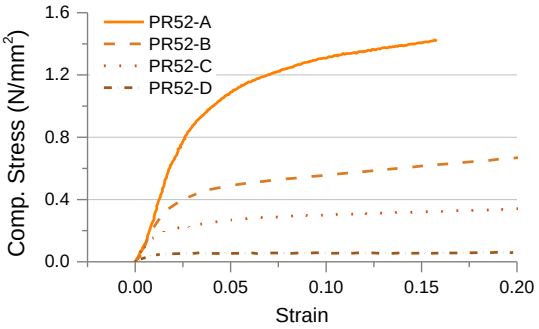

FIGURE 7: Compressive Strength

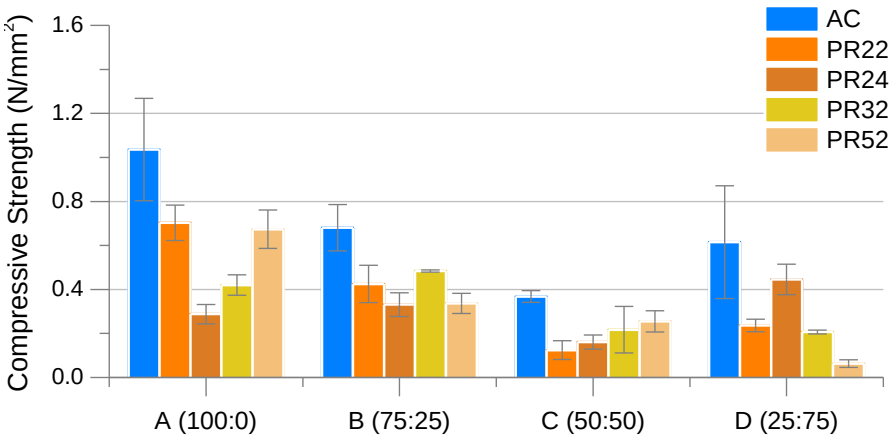

FIGURE 7 demonstrates that the resulting compressive strength values vary quite considerably with results ranging from 0.06 to 1.00 N/mm^2. Eleven out of the twenty specimens were found to fall within the typical range for low density rigid polymer foams (0.3 – 1.7 N/mm^2) (Ashby et al., 2013) with the AC samples appearing to offer the highest strength values. These AC samples provided statistically significant improvements over most of the other alginate types with the exceptions of PR32 and PR52 in batch C and PR24 in batch D. The highest strength value was obtained for the alginate only sample and in general strength was found to decrease when the proportion of alginate was replaced with clay down to a ratio of 50:50. Interestingly, the D sample which consisted mainly of the clay with only a 25% dosage of alginate, achieved similar results to the 50:50 mix, although the high variability of results should again be noted. PR22 follows a similar pattern to AC with the alginate only sample offering the highest strength whilst lower values were observed for the lower polymer contents. In contrast, PR24 displays comparatively low strength values for the alginate only sample and the highest value was obtained when only 25% alginate is used. This is most likely due to the fact that the high viscosity PR24 samples result in poorer mixing during sample preparation with high polymer contents. This also explains the defects observed for PR24-A and PR24-B. With PR32 and PR52, the lowest strength results are observed with the lower polymer dosage and the 75:25 mix ratios offer the most favourable results from the alginate-clay mixes.

Overall the compressive strength results indicate that whilst the addition of alginate leads to improvements over the clay control samples, since these samples are too fragile to even be tested, the most effective alginate dosage is dependent upon the specific alginate product used. In considering ratios B, C and D, for the highest viscosity alginates (AC and PR24) an alginate content

of only 25% provides sufficient improvements. However, for the lower viscosity alginates (PR32 and PR52), better results are achieved with 75% alginate. Furthermore, in terms of alginate composition, as shown in TABLE 1, PR24 has a much greater G content than the other products which suggests a greater capacity for crosslinking with calcium. This may explain why PR24 performs better when there is an increased quantity of clay.

When comparing the results to other similar studies, although other studies report increasing strength values with increasing polymer content (Ohta and Nakazawa, 1995), this is only visible for some alginate types in our study. The compressive strength values for the 50:50 mixes are generally lower than for the comparable 50% starch: 50%clay aerogel (Ohta and Nakazawa, 1995) which achieves a compressive strength value of 0.5 N/mm^2.

3.2.2. Modulus of Elasticity

In comparing the modulus of elasticity values, again results vary depending on the alginate type and dosage with average values ranging between 3 - 33 N/mm^2 (FIGURE 8). This is slightly lower than the range for typical polymer foams (23 – 80 N/mm^2) and more comparable to a natural material like cork (Ashby et al., 2013). However the results for AC-C, PR22-C and PR32-C which fall within the 5 – 10 N/mm^2 range are similar to the modulus range of 4 – 7 N/mm^2 reported for PVOH-clay aerogel (Wang et al., 2013) and that of ~6 N/mm^2 for a 50:50 alginate-clay aerogel (Chen et al., 2012).

FIGURE 8: Modulus of Elasticity

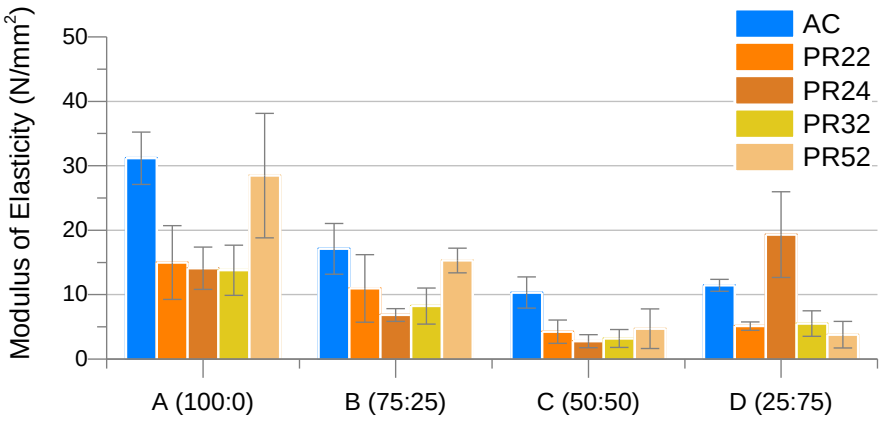

293 It should be noted that Chen et al.'s (2012) results also showed a general decrease in modulus values
294 with decreasing alginate content. This trend is apparent for AC, PR22, PR32 and PR52 although
295 slight increases may be observed for the lowest alginate content (D). The exception to this is PR24
296 where the D sample is greater than all of the other mix ratios. Again it is possible in this case that the
297 high viscosity and presence of air voids is leading to poorer rigidity but this can be improved by
298 increasing the proportion of clay. The particularly high value exhibited by PR24-D compared to the
299 same mix ratio for the other alginate types further highlights the importance of the G content when
300 sufficient quantities of clay are present.

301

302 **3.3. Microstructure**

303 **3.3.1. SEM Analysis**

304 SEM images are displayed in FIGURE 9 to FIGURE 14 at a magnification of 500x. These show the
305 porous structures obtained as a result of the sublimation of the ice crystals. Most of the samples were
306 highly heterogeneous across the fracture surface highlighting that the overall microstructure was not
307 uniform. This can be partly explained by the freezing process since the cell morphology is largely
308 governed by the ice crystal growth which is in turn dependent on the freezing temperature, rate and
309 direction of heat flow (O'Brien et al., 2004; Wang et al., 2013). In this case whilst the same flash
310 freezing method was adopted for all samples, there is still limited control of the kinetics of ice crystal
311 growth. Therefore although attempts have been made to obtain images of the cross-sections of the
312 resulting pores (i.e. perpendicular to the main solidification direction) this could not always be
313 guaranteed. It is therefore difficult to make definitive conclusions from some of the resulting images in
314 terms of quantitative analysis (e.g. mean cell dimensions and cell wall thickness). Nevertheless, some
315 general qualitative observations are offered.

316 In firstly considering, the neat alginate samples (A), the structures are fairly disordered consisting of
317 parallel sheets with relatively thick cell walls. These observations are similar to the irregular
318 topography described by Cheng et al. (2012) for sodium alginate aerogels. However, the pure clay
319 sample (FIGURE 14) displays a distinct lamellar structure, similar to the linear pore structure
320 observed by Nakazawa et al. (1987) for 10 wt% bentonite aerogels. It has been reported that an

increase in viscosity can retard ice crystal growth meaning that a higher molecular weight polymer, increased polymer concentration or increased level of cross-linking could increase the likelihood of a cellular, network structure rather than lamellar morphology (Gawryla et al., 2008; Chen et al. 2012). From the images presented here for the composite materials (mix ratios B, C & D), both types of structure are visible.

FIGURE 9: SEM Micrographs - AC

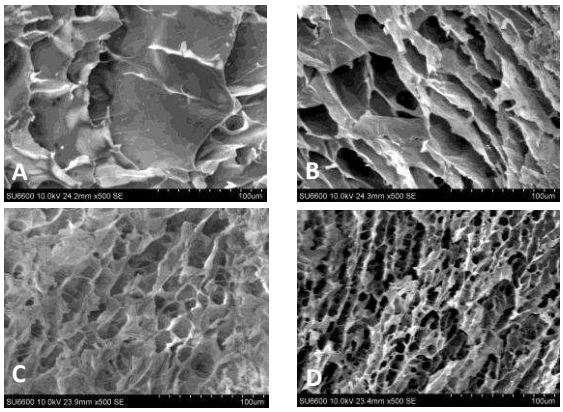

FIGURE 10: SEM Micrographs – PR22

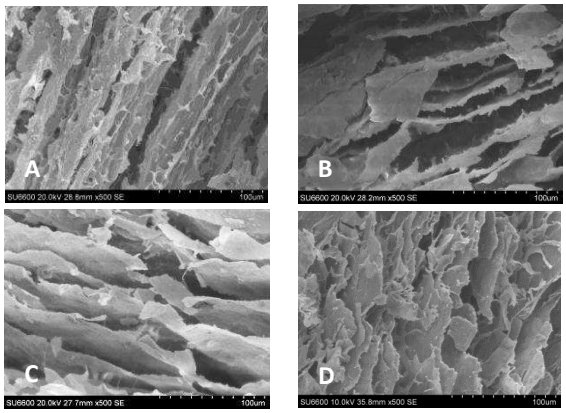

FIGURE 11: SEM Micrographs – PR24

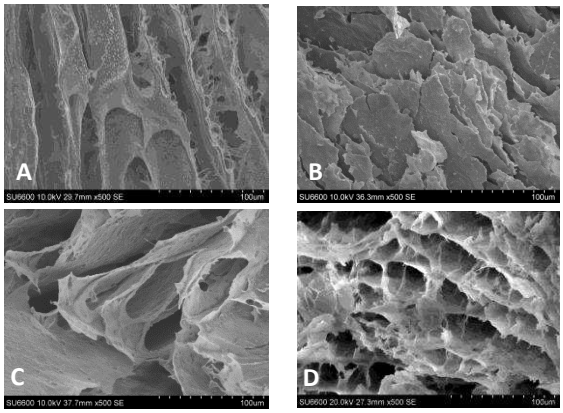

FIGURE 12: SEM Micrographs – PR32

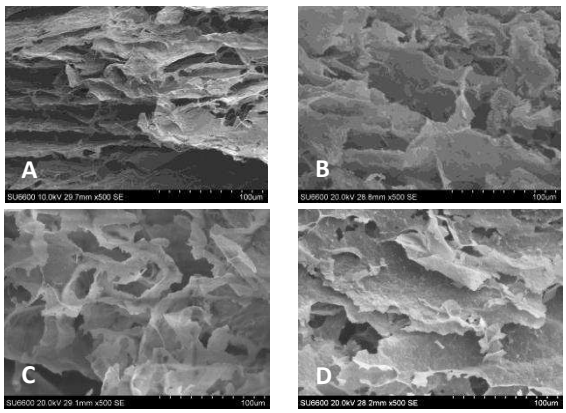

FIGURE 13: SEM Micrographs – PR52

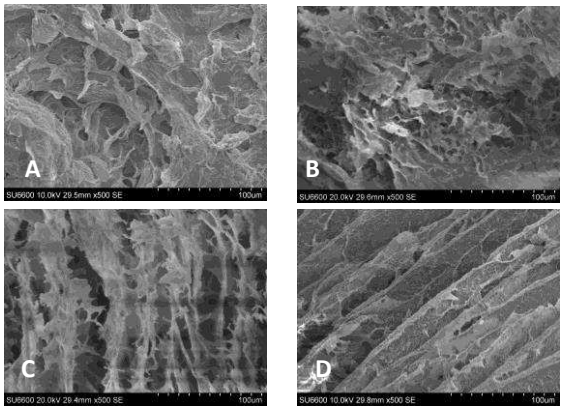

FIGURE 14: SEM Micrographs – Clay (E)

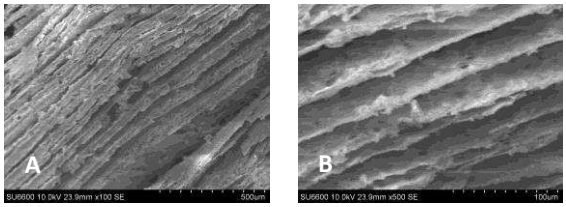

Relating these observations to the results of the mechanical testing, the formation of a network structure with small cells can help to reduced local stress and can therefore be linked to higher compressive strengths and higher modulus values (Svagan et al., 2011; Wang, 2015). Given that this type of structure is particularly apparent in AC-C, AC-D and PR22-D, this may explain the relatively good strength characteristics of these samples despite their low polymer content. These observations also support work by Chen et al. (2012) where the addition of montmorillonite clay was also found to transform the distinct layered morphology of an alginate aerogel to a co-continuous network which consequently improved the mechanical properties. Gawryla et al. (2008) also describe this shift in casein-clay aerogels whereby the separated layers change to a network structure whereby the layers are connected by a polymer web. This web-like structure reportedly helps to increase the isotropy of the material, meaning that it its less influenced by the size or direction the ice crystal growth.

On the other hand, the system viscosity can also have detrimental effect on the aerogel microstructure (Pojanavaraphan et al., 2010). This can lead to the entrapment of air resulting in the formation of spherical voids within the internal structure (Gawryla et al., 2008). For the alginate-clay aerogels, in addition to the macroscopic air bubbles highlighted as part of the visual observations, evidence of these types of defects were also found in the SEM micrographs. It should be acknowledged that the links between the complex variables involved in the ice-templating process and the resulting morphologies, which are in turn linked to the distribution of local stresses and mechanical response, are still not fully understood (Svagan et al., 2011 ;Li et al., 2012; Deville et al., 2016). However these structural defects will clearly have an impact on the structural properties and may explain the high variations in compressive strength and modulus reported.

3.3.2. Porosity

Given that the air pores in the aerogel samples are created from the ice crystals formed during freezing, it would be expected that the porosity of the aerogels would be dependent on the volume of water. Since all of the samples are 10 wt% solids, the total theoretical porosity should be close to 90%. For the calculated porosities, which are based on the sample weights and volumes, the values range from 93% to 96%. These are close to the values for other polymer-clay aerogels produced using the

same solids content. For example Wang (2015) quotes a porosity of around 94% for PVOH-clay aerogels whilst Longo et al. (2013) describe values of close to 90% for PS-clay composites.

TABLE 4: Estimated Porosity (Alginate Dosage)

Alg:Clay	**AC-A (100:0)**	**AC-B (75:25)**	**AC-C (50:50)**	**AC-D (25:75)**	**E (0:100)**
Bulk Density (g/cm^3)	0.097	0.097	0.076	0.104	0.090
Alginate particle density (g/cm^3)	1.59	1.1925	0.795	0.3975	0
Clay particle density (g/cm^3)	0	0.625	1.25	1.875	2.5
Total Porosity	92.7%	94.6%	94.3%	95.6%	96.4%

TABLE 5: Estimated Porosity (Alginate Type)

Alg:Clay	**AC-C** (50:50)	**PR22-C** (50:50)	**PR24-C** (50:50)	**PR32-C** (50:50)	**PR52-C** (50:50)
Bulk Density (g/cm^3)	0.0759	0.0851	0.0349	0.1193	0.1309
Alginate particle density (g/cm^3)	0.795	0.795	0.795	0.795	0.795
Clay particle density (g/cm^3)	1.25	1.25	1.25	1.25	1.25
Total Porosity	94.3%	95.8%	98.3%	94.2%	93.6%

While these high porosity values point towards good thermal performance given the estimated volume of air, it is acknowledged that a further investigation of the thermal properties would be required in order to make a clearer comparison with other insulation materials. As previously discussed, thermal conductivities of 0.2 – 0.4 W/m-K would need to be achieved in order to compete with conventional materials (e.g. mineral or polymer based products) while values below 0.2 W/m-K would be required for use in high-performance applications.

4.4. Cost and Environmental Impacts

The results from the cost modelling calculations, based on estimated material and production costs from the aerogel prototypes are presented in TABLE 6. These estimates are based on the purchase costs and required quantities of the individual materials (from MBL or other suppliers) and calculated electricity costs based on equipment power consumption and duration of use. The material costs vary marginally depending upon the mix ratio used and based on these estimates, due the higher costs of clay (£20/kg) and slight differences in costs for the Laminaria Hyperborea (LH) species (£11/kg) and the Acsophyllum Nodosum (AN) product (£8.50/kg). In terms of production, the greatest cost is associated with the freeze-drying and the electricity consumed during this process, however these costs are similar to the material costs. In total this gives estimated production costs of approximately £3 per 100 cm^3 sample.

TABLE 6: Cost Estimations

Prototype Samples		**£/100cm^3**
Materials	Alginate, Clay, Liquid N_2	£1.62 - £1.69
Processing	Electricity (Mixing & Freeze-drying)	£1.46
Total		**£3.08- £3.15**

These cost calculations are based on laboratory scale equipment however it is acknowledged that for commercial production, larger and more cost efficient practices would be adopted. Simply extrapolating the costs of the small samples gives a figure of £308 - £315 per kg or £616 - 630 per m^2 assuming that in volumetric terms that the material could be formed into a 20mm thick panel. This of course excludes other overheads associated with full scale production however still highlights the high costs involve even in the basic material and drying requirements. For larger scale production, the main disadvantage is the cost of the liquid nitrogen since the mass of liquid nitrogen required can equate to more than 3 times the mass of the material being frozen (Smith, 2011). In terms of drying, again assuming the use of an industrial scale freeze-dryer such as those used within the food industry, it would be anticipated that cost savings could be achieved compared to the laboratory scale dryer. Although in comparison with air-drying, the cost of freeze-drying can be 4-8 times more expensive (Ratti, 2001), there are on-going efforts to increase the efficiency and energy demands of the freeze-drying process which should help to reduce costs in future (Liu et al., 2008).

Furthermore, other studies regarding clay-based aerogels have reported that it is the use of freeze-drying as an alternative to the relatively expensive solvent exchange and autoclave drying required for silica aerogels which helps to keep the manufacturing costs low (Schiraldi et al., 2010). Indeed Dalton et al. (2010) give an estimated cost of £200 per m^3 for their clay-polymer product which uses a similar production process to the aerogels produced in this study. If these production costs could be achieved, on a m^2 basis a clay-polymer aerogel would therefore be much less than for a silica aerogel blanket which can cost between £24 - 174/m^2, depending on product thickness. A recent study in the UK quoted costs of around £50/m^2 for a 40mm Spacetherm® product (BRE, 2016). This is more than double the cost of a polymer based insulation like PUR and around 7 times greater than rockwool insulation (BRE, 2016). The estimated costs for the clay-polymer aerogel would therefore be more comparable to conventional insulations which are typically below £20/m^2 (BRE, 2016). All costs must

405 however also be weighed against the potential long term cost savings in relation to reduced heat
406 losses, and the advantages of aerogels with regards to the reduced thicknesses required.

407 In considering the environmental analysis of the aerogels, the embodied energy of the alginate, based
408 on production data from the supplier (MBL) equates to 8.5 and 6.7 MJ/kg of dry alginate product for
409 the LH and AN products respectively (TABLE 7). It should be noted that these values are lower than
410 that of the value for 'algae' (20 MJ/kg) used by Galán-Marín et al. (2015) for other composite clay-
411 alginate materials. This 'algae' data, sourced from Resurreccion et al. (2012), relates to cultivated
412 micro-algae for biofuel production and therefore requires very different energy and resource inputs to
413 alginate produced from natural seaweed. It is therefore not surprising that there is a discrepancy with
414 the embodied energy values given in the two studies. Compared to other polymers which are typically
415 used in clay-polymer aerogels, PVOH for example, which is used in the aerogels described by Bandi
416 and Schiraldi (2006) and Hostler et al. (2009), is reported to have an embodied energy of 60 to 100
417 MJ per kg (Patel et al., 2003). Other polymers used in clay aerogels include natural rubber
418 (Pojanavaraphan et al., 2010b) and epoxy resins (Arndt et al., 2007) which have an embodied energy
419 of 73 MJ/kg and 137 MJ/kg respectively (Hammond and Jones, 2011). Provided that the rest of the
420 production process is identical, an alginate –based aerogel would have less of an environmental
421 impact than these other clay-polymer aerogels. For the clay component, the process for obtaining
422 this material typically involves either hydraulic mining or open pit extraction followed by purifying,
423 drying, milling, packaging and transport (Heath et al., 2014). Embodied energy and embodied CO_2
424 values quoted for bentonite, such as those used by Brandt (2015), are 0.4 MJ/kg and 0.031 kg CO_2/kg.
425 These are not dissimilar to the equivalent values for other quarried materials like soil, perlite and
426 vermiculite (Hammond and Jones, 2011).

TABLE 7: Embodied Energy (Alginate)

Process		**Laminaria Hyperborea** MJ/kg	**Ascophyllum Nodosum** MJ/kg	**Laminaria Hyperborea** (kg CO_2e/kg)	**Ascophyllum Nodosum** (kg CO_2e/kg)
Harvesting	Transport from harvest site to dock	3.10	2.07	0.23	0.16
	Cutting	2.36	1.57	0.18	0.12
Processing (Milling, centrifugation & drying)	Electrical Energy	0.01	0.01	0.00	0.00
	Latent Heat (Fluid Bed Dryer)	0.05	0.05	0.00	0.00
	Sensible Heat	0.02	0.02	0.00	0.00
Water	Washing/ processing	2.93	2.93	0.10	0.10

	Total	**8.47**	**6.65**	**0.51**	**0.38**

All energy data based on estimates provided by MBL

Aside from the environmental impacts of the materials, the energy requirements associated with the production processes must also be considered. In considering firstly the freezing process, as per the cost modelling, one of the key aspects to consider is the use of liquid nitrogen (N_2) as significant amounts of energy are required in its production. Pušavec et al. (2009) for example quoted a value of 1.8 MJ/kg. Water is also used during the production of liquid nitrogen as a cooling fluid, although it is not physically consumed and can therefore be recycled/returned to the environment (Pušavec et al., 2009). Waste outputs are therefore minimal as the cooling water is non-toxic and no CO or SO is produced. According to Ratti (2001), in terms of the overall freeze-drying process, the freezing stage equates to only 4% of the total energy consumption, whilst the sublimation element accounts for around 45%. Overall the energy required to remove 1 kg of water by way of freeze-drying is nearly double of that required using conventional drying methods (Liu et al., 2008). Nonetheless compared to other supercritical drying methods, such as those involving CO_2, it has been argued that freeze-drying offers a more environmentally benign alternative (Schiraldi et al., 2010). There is however currently a lack of evidence to support this since a comprehensive LCA for freeze-dried aerogels has yet to be conducted. In fact, according to a recent study regarding drying methods for foodstuffs (Hofland, 2014), supercritical drying with CO_2 was shown to consume less energy than freeze-drying. Lower embodied CO_2 values of 5 kg CO_2 /kg dried product were also reported by Hofland (2014) for the CO_2 methods compared to of 30 kg CO_2 /kg for freeze-drying.

Based on the production processes used in this study, estimates regarding the energy inputs for the laboratory scale prototypes are illustrated in TABLE 8. These are also converted to embodied CO_2 values in TABLE 9 using the relevant conversion factors (Hill et al., 2013; DECC, 2016). As expected, the greatest energy input is that of the drying phase which constitutes over 90% of the total, meaning that differences between mix ratios are considered minor. The resulting embodied energy estimate of 54 MJ per 100cm^3 batch of material is similar to the value of 29 MJ per 40cm^3 calculated by Dowson et al. (2012) for a high-temperature supercritically dried (HTSD) silica aerogel and lower than that of a low-temperature supercritically dried (LTSD) silica materials (63 MJ per 40cm^3 batch). The estimated

embodied CO_2 value of 6.2 kg CO_2 per 100cm^3 is also higher than that of the HTSD aerogel (0.73 kg CO_2 per 40cm^3) but lower than the value of 6.63 kg CO_2 per 40cm^3 quoted for the LTSD aerogel.

TABLE 8: Embodied Energy

Materials	**Embodied Energy** (MJ/kg)	**Quantity** (kg/ kg)	**Total = EE x Quantity** (MJ/kg)
Alginate	6.65 – 8.47 [a]	0.25 – 0.75	1.66 – 6.35
Bentonite	0.40 [b]	0.25 – 0.75	0.10 - 0. 03
Liquid Nitrogen	1.80 [c]	100	180
Water	0.01 [d]	9	0.09
Process	**Electricity** (kWh/kg)	**Electricity** (MJ/kg)	**Total** (MJ/kg)
Mixing	18	64.8	64.8
Freeze-drying	1440	5184	5184
Total (MJ/kg)			**5395 – 5399**
Total (MJ/100 cm^3)			**54.0**

a - from Table 7, b –Brandt (2015), c –Pusavec et al. (2010)
d - Hammond and Jones (2011)

TABLE 9: Embodied CO_2

Materials	**Embodied CO_2** (kg CO2e / kg)	**Quantity** (kg/ kg)	**Total = EE x Quantity** (MJ/kg)
Alginate	0.37 – 0.51 [a]	0.25 – 0.75	0.09 – 0.38
Bentonite	0.03 [b]	0.25 – 0.75	0.01 – 0.02
Liquid Nitrogen	0.21 [c]	100	21
Water	0.001 [d]	9	0.01
Process	**Electricity** (kWh/kg)	**Conversion factor** [e]	**Total = Electricity x conversion factor** (kg CO_2 e/kg)
Mixing	18	0.41	7.38
Freeze-drying	1440	0.41	590.4
Total (MJ/kg)			**618.89 – 619.19**
Total (MJ/100 cm^3)			**6.2**

a - from Table 7, b – from Ecoinvent (Brandt, 2015), c – Pusavec et al. (2010), d - from Hammond and Jones (2011) , e – DECC (2016)

It should be noted that the calculations for the alginate-clay prototypes are also based on laboratory scale equipment and so energy-efficiency savings would be expected for larger scale production. Indeed Dowson et al. (2012) demonstrated that basic scaling revisions between laboratory scale samples and industrial production involving larger batches could lead to an embodied energy reduction of around two thirds with a similar reduction on the CO_2 burden. If similar savings could be achieved for the clay-aerogel samples, this would give approximate values of below 18 MJ/100 cm^3 and 2.3 kg CO_2/100cm^3. Whilst these are relatively high compared to a commercial silica aerogel blanket (Spacetherm = 0.8 MJ/100 cm^3) it should also be noted that the calculation for this product is

based on a composite blanket and therefore inclusive of fibres rather than the pure aerogel. Furthermore these estimations are also related to the embodied energy per functional unit rather than the equivalent amount of material required in order to achieve a given U-value. For example, in comparing the thermal performance of different insulators, Dalton et al. (2010) report that a clay polymer aerogel could be half the thickness of a silica aerogel blanket or a quarter the thickness of and EPC board and achieve an equivalent U-value. Assuming that the thermal conductivity of the alginate-clay aerogel would be similar to that of the clay-polymer aerogels described by Dalton et al. (2010), it is likely that mass of material required would also be less than for conventional insulations. This would have an impact on the overall embodied energy and costs. Further investigation of thermal properties would however be required in order to evaluate the proposed material and compare with the performance of existing products. This will require moving beyond the small scale prototype samples to larger test pieces. The impact of moisture conditions and temperature on thermal performance would also need to be considered.

5. CONCLUSIONS

In the past decade, high performance insulations such as aerogels have emerged as alternatives to conventional insulating materials and have the potential to reduce heat losses in buildings, particularly in retrofit scenarios where minimum product thicknesses are desirable. Although the high costs of aerogel insulations still hinder their widespread use, strategies to reduce their processing costs and make use of lower cost raw materials, will likely make aerogels more affordable in the future and hence increase the commercial viability of using such materials in bulk applications like building insulation. Furthermore, the use of renewable materials such as biopolymers has been identified as an important strategy in improving the whole life cycle environmental performance and reducing the overall environmental impacts.

In this study, clay-alginate aerogels have been investigated as a more environmentally friendly and potentially more economical alternative to existing silica based aerogels. It has been demonstrated that various types of sodium alginate can be added to bentonite clay in order to improve the strength of the aerogels. The small-scale prototypes produced have a low bulk density with mechanical properties similar to other polymer-based foams. It has also been demonstrated that the optimum mix

ratio is dependent on the type of alginate used with both polymer viscosity and composition having an effect on potential bonding mechanisms and interactions with the clay. Indeed significant differences in compressive strength, modulus of elasticity and microstructure have been observed in specimens with the same mix proportions and similar bulk densities where the only variable is the alginate source.

With regards to economic viability, whilst the calculations based on laboratory scale production were found to be high, the majority of costs were associated with freeze-drying element owing to the high cost of liquid N_2 and the electricity consumption required during the drying phase. However, since aerogels are still a developing technology, many of these processing techniques are still being investigated and developed for larger scale production and so it is anticipated that these costs will be reduced with scaling revisions. In terms of the environmental impacts of the material, the embodied energy values for the proposed alginate-clay aerogel are much higher than that of existing silica aerogel blankets. Even assuming the aforementioned scaling revisions are applied, the embodied energy of the aerogel product is still over 10 times greater than commercially available silica aerogel blankets. It can therefore not be assumed that the use of natural, renewable materials or freeze-drying methods will guarantee superior environmental performance compared to silica-based aerogels. Given that that these comparisons are based on extrapolated values and estimated thermal properties, a more detailed analysis involving the specific thermal conductivity values and more accurate production data would shed further light on the environmental performance. A further investigation of the hygrothermal behavior of the samples using larger prototypes would therefore be required in order to fully assess the commercial viability.

Overall these clay-alginate aerogels have the potential to be used as insulating materials within building, further research into both their specific material properties and appropriate production methods is required in order to fully assess their technical and commercial viability. Other ongoing work is currently investigating a wider range of alginate types as well as alternatives clays and additional calcium sources. In order to fully assess the suitability of clay-alginate aerogels as a potential insulation material, comparison of other technical properties such as porosity and thermal conductivity is recommended for future research.

ACKNOWLEDGEMENTS

The author wishes to thank the funding providers for the project including the University of Strathclyde, the Energy Technology Partnership and Marine Biopolymers Ltd. Acknowledgement is also made to the Advanced Materials Research Lab and the Chemical Processing and Engineering Department at the University of Strathclyde where the experimental work was conducted.

References

Alam, M., Singh, H., Limbachiya, M.C., 2011. Vacuum Insulation Panels (VIPs) for building construction industry – A review of the contemporary developments and future directions. Appl. Energy 88, 3592–3602. https://doi.org/10.1016/j.apenergy.2011.04.040

Arndt, E.M., Gawryla, M.D., Schiraldi, D.A., 2007. Elastic, low density epoxy/clay aerogel composites. J. Mater. Chem. 17, 3525–3529.

Ashby, M.F., Shercliff, H., Cebon, D., 2013. Materials: engineering, science, processing and design, 3rd ed. Butterworth-Heinemann, Oxford.

Aspen Aerogels, 2011. Datasheet Spaceloft® High Performance Insulation for Building Envelopes [WWW Document]. URL http://www.tcnano-norge.no/Spaceloft_10_A2_REV1.pdf (accessed 6.29.15).

Aspinall, G.O., 2014. The polysaccharides. Academic Press Inc., New York.

Baetens, R., Jelle, B.P., Gustavsen, A., 2011. Aerogel insulation for building applications: A state-of-the-art review. Energy Build. 43, 761–769. https://doi.org/10.1016/j.enbuild.2010.12.012

Bandi, S., Schiraldi, D.A., 2006. Glass transition behavior of clay aerogel/poly (vinyl alcohol) composites. Macromolecules 39, 6537–6545.

Biswas, K., Shrestha, S.S., Bhandari, M.S., Desjarlais, A.O., 2016. Insulation materials for commercial buildings in North America: An assessment of lifetime energy and environmental impacts. Energy Build. 112, 256–269. https://doi.org/10.1016/j.enbuild.2015.12.013

Brandt, A.R., 2015. Embodied Energy and GHG Emissions from Material Use in Conventional and Unconventional Oil and Gas Operations. Environ. Sci. Technol. 49, 13059–13066. https://doi.org/10.1021/acs.est.5b03540

BRE, 2016. Rethinking refurbishment: Todmorden and Nelson [WWW Document]. URL http://www.bre.co.uk/filelibrary/victorian_terrace/pdfs/BRE5776Elevate&Calder-e.pdf (accessed 6.1.16).

Buratti, C., Merli, F., Moretti, E., 2017. Aerogel-based materials for building applications: Influence of granule size on thermal and acoustic performance. Energy Build. 152, 472–482. https://doi.org/10.1016/j.enbuild.2017.07.071

Carbon Trust, 2012. Building fabric: Energy saving techniques to improve the efficiency of building structures (No. CTV069).

Chen, H., Wang, Y., Sánchez-Soto, M., Schiraldi, D., 2012. Low flammability, foam-like materials based on ammonium alginate and sodium montmorillonite clay. Polymer 53, 5825–5831. https://doi.org/http://dx.doi.org/10.1016/j.polymer.2012.10.029

Chen, H.-B., Hollinger, E., Wang, Y.-Z., Schiraldi, D.A., 2014. Facile fabrication of poly(vinyl alcohol) gels and derivative aerogels. Polymer 55, 380–384. https://doi.org/10.1016/j.polymer.2013.07.078

Cheng, Y., Lu, L., Zhang, W., Shi, J., Cao, Y., 2012. Reinforced low density alginate-based aerogels: Preparation, hydrophobic modification and characterization. Carbohydr. Polym. 88, 1093–1099. https://doi.org/10.1016/j.carbpol.2012.01.075

Cuce, E., Cuce, P.M., Wood, C.J., Riffat, S.B., 2014. Toward aerogel based thermal superinsulation in buildings: A comprehensive review. Renew. Sustain. Energy Rev. 34, 273–299.

Dalton, J.C., Brase, A., Kuo, N., Marzano, M., 2010. Evacuated Panels Utilizing Clay-Polymer Aerogel Composites for Improved Housing Insulation. Case Western Reserve University.

Davis, T.A., Llanes, F., Volesky, B., Diaz-Pulido, G., McCook, L., Mucci, A., 2003. 1H-NMR study of Na alginates extracted from Sargassum spp. in relation to metal biosorption. Appl. Biochem. Biotechnol. 110, 75–90.

DECC, 2016. UK Government GHG Conversion Factors for Company Reporting.

579 Deville, S., Meille, S., Seuba, J., 2016. A meta-analysis of the mechanical properties of ice-templated
580 ceramics and metals. Sci. Technol. Adv. Mater.
581 Dowson, M., Grogan, M., Birks, T., Harrison, D., Craig, S., 2012. Streamlined life cycle assessment of
582 transparent silica aerogel made by supercritical drying. Appl. Energy 97, 396–404.
583 Draget, K.I., Skjåk-Bræk, G., Stokke, B.T., 2006. Similarities and differences between alginic acid gels
584 and ionically crosslinked alginate gels. 7th Int. Hydrocoll. Conf. 20, 170–175.
585 https://doi.org/10.1016/j.foodhyd.2004.03.009
586 Druel, L., Bardl, R., Vorwerg, W., Budtova, T., 2017. Starch Aerogels: A Member of the Family of
587 Thermal Superinsulating Materials. Biomacromolecules 18, 4232–4239.
588 Felton, D., Fuller, R., Crawford, R.H., 2013. The potential for renewable materials to reduce the
589 embodied energy and associated greenhouse gas emissions of medium-rise buildings. Archit.
590 Sci. Rev. 1–8. https://doi.org/10.1080/00038628.2013.829022
591 Finlay, K., Gawryla, M.D., Schiraldi, D.A., 2007. Biologically Based Fiber-Reinforced/Clay Aerogel
592 Composites. Ind. Eng. Chem. Res. 47, 615–619. https://doi.org/10.1021/ie0705406
593 Funami, T., Fang, Y., Noda, S., Ishihara, S., Nakauma, M., Draget, K.I., Nishinari, K., Phillips, G.O.,
594 2009. Rheological properties of sodium alginate in an aqueous system during gelation in
595 relation to supermolecular structures and Ca2+ binding. Food Hydrocoll. 23, 1746–1755.
596 https://doi.org/10.1016/j.foodhyd.2009.02.014
597 Galán-Marín, C., Rivera-Gómez, C., García-Martínez, A., 2015. Embodied energy of conventional
598 load-bearing walls versus natural stabilized earth blocks. Energy Build. 97, 146–154.
599 https://doi.org/10.1016/j.enbuild.2015.03.054
600 Gawryla, M.D., Nezamzadeh, M., Schiraldi, D.A., 2008. Foam-like materials produced from abundant
601 natural resources. Green Chem. 10, 1078–1081.
602 Grasdalen, H., Larsen, B., Smidsrød, O., 1979. A p.m.r. study of the composition and sequence of
603 uronate residues in alginates. Carbohydr. Res. 68, 23–31. https://doi.org/10.1016/S0008-
604 6215(00)84051-3
605 Hammond, G., Jones, C., 2011. Inventory of Carbon & Energy Version 2.0 (ICE V2. 0). Dep. Mech.
606 Eng. Univ. Bath Bath UK.
607 Heath, A., Paine, K., McManus, M., 2014. Minimising the global warming potential of clay based
608 geopolymers. J. Clean. Prod. 78, 75–83.
609 Hill, N., Venfield, H., Dun, C., James, K., 2013. Government GHG conversion factors for company
610 reporting: methodology paper for emission factors. DEFRA DECC.
611 Hofland, G., 2014. Preserving Raw materials Into Excellent and Sustainable End Products While
612 Remaining Fresh (No. 245280).
613 Hostler, S.R., Abramson, A.R., Gawryla, M.D., Bandi, S.A., Schiraldi, D.A., 2009. Thermal conductivity
614 of a clay-based aerogel. Int. J. Heat Mass Transf. 52, 665–669.
615 https://doi.org/10.1016/j.ijheatmasstransfer.2008.07.002
616 Jelle, B.P., 2011. Traditional, state-of-the-art and future thermal building insulation materials and
617 solutions – Properties, requirements and possibilities. Energy Build. 43, 2549–2563.
618 https://doi.org/10.1016/j.enbuild.2011.05.015
619 Kingspan, 2011. Kingspan Thermawall TW50 Partial Fill Cavity Wall Insulation [WWW Document].
620 URL http://www.kingspaninsulation.co.uk/getattachment/b08c2d53-474b-4bfd-ad44-
621 d38eb4041dd2/Thermawall-TW50.aspx (accessed 6.29.15).
622 Kiss, B., Manchón, C.G., Neij, L., 2013. The role of policy instruments in supporting the development
623 of mineral wool insulation in Germany, Sweden and the United Kingdom. Environ. Manag.
624 Sustain. Univ. EMSU 2010 Eur. Roundtable Sustain. Consum. Prod. ERSCP 2010 48, 187–
625 199. https://doi.org/10.1016/j.jclepro.2012.12.016
626 Kistler, S.S., 1934. The Relation between Heat Conductivity and Structure in Silica Aerogel. J. Phys.
627 Chem. 39, 79–86. https://doi.org/10.1021/j150361a006
628 Kistler, S.S., 1932. Coherent Expanded Aerogels. J. Phys. Chem. 36, 52–64.
629 Kogel, J.E., Trivedi, N.C., Barker, J.M. (Eds.), 2006. Industrial minerals & rocks: commodities,
630 markets, and uses. Society for Mining Metallurgy & Exploration, Colorado, USA.
631 Korjenic, A., Petránek, V., Zach, J., Hroudová, J., 2011. Development and performance evaluation of
632 natural thermal-insulation materials composed of renewable resources. Energy Build. 43,
633 2518–2523. https://doi.org/10.1016/j.enbuild.2011.06.012
634 Li, W., Lu, K., Walz, J., 2012. Freeze casting of porous materials: review of critical factors in
635 microstructure evolution. Int. Mater. Rev. 57, 37–60.
636 Liang, Y., Wu, H., Huang, G., Yang, J., Ding, Y., 2017a. Prediction and Optimization of Thermal
637 Conductivity of Vacuum Insulation Panels with Aerogel Composite Cores. 10th Int. Symp.

638 Heat. Vent. Air Cond. ISHVAC2017 19-22 Oct. 2017 Jinan China 205, 2855–2862.
639 https://doi.org/10.1016/j.proeng.2017.09.909
640 Liang, Y., Wu, H., Huang, G., Yang, J., Wang, H., 2017b. Thermal performance and service life of
641 vacuum insulation panels with aerogel composite cores. Energy Build. 154, 606–617.
642 https://doi.org/10.1016/j.enbuild.2017.08.085
643 Liu, X., Qian, L., Shu, T., Tong, Z., 2003. Rheology characterization of sol–gel transition in aqueous
644 alginate solutions induced by calcium cations through in situ release. Polymer 44, 407–412.
645 https://doi.org/10.1016/S0032-3861(02)00771-1
646 Liu, Y., Zhao, Y., Feng, X., 2008. Exergy analysis for a freeze-drying process. Appl. Therm. Eng. 28,
647 675–690. https://doi.org/10.1016/j.applthermaleng.2007.06.004
648 Lolli, N., Hestnes, A.G., 2014. The influence of different electricity-to-emissions conversion factors on
649 the choice of insulation materials. Energy Build. 85, 362–373.
650 https://doi.org/10.1016/j.enbuild.2014.09.042
651 Longo, S., Mauro, M., Daniel, C., Galimberti, M., Guerra, G., 2013. Clay exfoliation and polymer/clay
652 aerogels by supercritical carbon dioxide. Front. Chem. 1.
653 https://doi.org/10.3389/fchem.2013.00028
654 Lopez Hurtado, P., Rouilly, A., Vandenbossche, V., Raynaud, C., 2016. A review on the properties of
655 cellulose fibre insulation. Build. Environ. 96, 170–177.
656 https://doi.org/10.1016/j.buildenv.2015.09.031
657 Madyan, O.A., Fan, M., Feo, L., Hui, D., 2016. Physical properties of clay aerogel composites: An
658 overview. Compos. Part B Eng. 102, 29–37.
659 https://doi.org/10.1016/j.compositesb.2016.06.057
660 Martinez, R.G., 2017. Highly Insulated Systems for Energy Retrofitting of Façades on its Interior.
661 Sustain. Synerg. Build. Urban Scale 38, 3–10. https://doi.org/10.1016/j.proenv.2017.03.065
662 Martins, M., Barros, A.A., Quraishi, S., Gurikov, P., Raman, S.P., Smirnova, I., Duarte, A.R.C., Reis,
663 R.L., 2015. Preparation of macroporous alginate-based aerogels for biomedical applications.
664 J. Supercrit. Fluids. https://doi.org/10.1016/j.supflu.2015.05.010
665 Martinsen, A., Skjåk-Bræk, G., Smidsrød, O., 1989. Alginate as immobilization material: I. Correlation
666 between chemical and physical properties of alginate gel beads. Biotechnol. Bioeng. 33, 79–
667 89.
668 McHugh, D.J., 2003. A Guide to the Seaweed Industry. Food and Agriculture Organization of the
669 United Nations, Rome.
670 Nakazawa, H., Yamada, H., Fujita, T., Ito, Y., 1987. Texture control of clay-aerogel through the
671 crystallization process of ice. Clay Sci. 6, 269–276.
672 Nosrati, R.H., Berardi, U., 2018. Hygrothermal characteristics of aerogel-enhanced insulating
673 materials under different humidity and temperature conditions. Energy Build. 158, 698–711.
674 https://doi.org/10.1016/j.enbuild.2017.09.079
675 Nussinovitch, A., Velez-Silvestre, R., Peleg, M., 1993. Compressive characteristics of freeze-dried
676 agar and alginate gel sponges. Biotechnol. Prog. 9, 101–104.
677 https://doi.org/10.1021/bp00019a015
678 O'Brien, F.J., Harley, B.A., Yannas, I.V., Gibson, L., 2004. Influence of freezing rate on pore structure
679 in freeze-dried collagen-GAG scaffolds. Biomaterials 25, 1077–1086.
680 Ohta, S., Nakazawa, H., 1995. Porous clay-organic composites: Potential substitutes for polystyrene
681 foam. Appl. Clay Sci. 9, 425–431. https://doi.org/10.1016/0169-1317(95)00003-M
682 Papadopoulos, A.M., 2005. State of the art in thermal insulation materials and aims for future
683 developments. Energy Build. 37, 77–86. https://doi.org/10.1016/j.enbuild.2004.05.006
684 Patel, M., Bastioli, C., Marini, L., Würdinger, E., 2003. Environmental assessment of bio-based
685 polymers and natural fibres. Life-Cycle Assess. Bio-Based Polym. Nat. Fibres Chapter
686 "biopolymers 10.
687 Pedroso, M., de Brito, J., Silvestre, J.D., 2017. Characterization of eco-efficient acoustic insulation
688 materials (traditional and innovative). Constr. Build. Mater. 140, 221–228.
689 https://doi.org/10.1016/j.conbuildmat.2017.02.132
690 Pojanavaraphan, T., Magaraphan, R., Chiou, B.-S., Schiraldi, D.A., 2010a. Development of
691 Biodegradable Foamlike Materials Based on Casein and Sodium Montmorillonite Clay.
692 Biomacromolecules 11, 2640–2646. https://doi.org/10.1021/bm100615a
693 Pojanavaraphan, T., Schiraldi, D.A., Magaraphan, R., 2010b. Mechanical, rheological, and swelling
694 behavior of natural rubber/montmorillonite aerogels prepared by freeze-drying. Appl. Clay Sci.
695 50, 271–279. https://doi.org/10.1016/j.clay.2010.08.020

Proctor Group, 2015. Datasheet Spacetherm® Thermal Insulation [WWW Document]. URL http://www.proctorgroup.com/images/downloads/Thermal-Insulation/Spacetherm/Proctors%20-%20Spacetherm%20Datasheet.pdf (accessed 6.29.15).
Pušavec, F., Stoić, A., Kopač, J., 2009. The role of cryogenics in machining processes. Teh. Vjesn. 16, 3–9.
Rassis, D., Nussinovitch, A., Saguy, I.S., 2003. Tailor-made porous solid foods. Int. J. Food Sci. Technol. 32, 271–278.
Ratti, C., 2001. Hot air and freeze-drying of high-value foods: a review. J. Food Eng. 49, 311–319.
Rehm, B. (Ed.), 2009. Alginates: Biology and applications, Microbiology Monographs. Springer, London.
Resurreccion, E.P., Colosi, L.M., White, M.A., Clarens, A.F., 2012. Comparison of algae cultivation methods for bioenergy production using a combined life cycle assessment and life cycle costing approach. Adv. Biol. Waste Treat. Bioconversion Technol. 126, 298–306. https://doi.org/10.1016/j.biortech.2012.09.038
Riffat, S.B., Qiu, G., 2013. A review of state-of-the-art aerogel applications in buildings. Int. J. Low-Carbon Technol. 8, 1–6.
Savio, L., Bosia, D., Patrucco, A., Pennacchio, R., Piccablotto, G., Thiebat, F., 2018. Applications of Building Insulation Products Based on Natural Wool and Hemp Fibers, in: Advances in Natural Fibre Composites. Springer, pp. 237–247.
Scherer, G.W., 1998. Characterization of aerogels. Adv. Colloid Interface Sci. 76–77, 321–339. https://doi.org/10.1016/S0001-8686(98)00051-7
Schiavoni, S., Bianchi, F., Asdrubali, F., 2016. Insulation materials for the building sector: A review and comparative analysis. Renew. Sustain. Energy Rev. 62, 988–1011.
Schiraldi, D.A., Bandi, S.A., Gawryla, M.D., 2006. Progress in clay aerogel/polymer composite materials. Polym. Prepr. 47, 313.
Schiraldi, D.A., Gawryla, M.D., Alhassan, S., 2010. Clay Aerogel Composite Materials. Adv. Sci. Technol. 63, 147–151.
Smith, P.G., 2011. An Introduction to Food Process Engineering, 2nd ed, Food Science Text. Springer, USA.
Stahl, T., Brunner, S., Zimmermann, M., Ghazi Wakili, K., 2012. Thermo-hygric properties of a newly developed aerogel based insulation rendering for both exterior and interior applications. Energy Build. 44, 114–117. https://doi.org/10.1016/j.enbuild.2011.09.041
Stec, A.A., Hull, T.R., 2011. Assessment of the fire toxicity of building insulation materials. Energy Build. 43, 498–506. https://doi.org/10.1016/j.enbuild.2010.10.015
Straatmann, A., Borchard, W., 2003. Phase separation in calcium alginate gels. Eur. Biophys. J. 32, 412–417.
Sutton, A., Black, D., Walker, P., 2011. Natural Fibre Insulation: An introduction to low-impact building materials (Information Paper No. (IP 18/11)). BRE Ltd.
Svagan, A.J., Berglund, L.A., Jensen, P., 2011. Cellulose Nanocomposite Biopolymer Foam: Hierarchical Structure Effects on Energy Absorption. ACS Appl. Mater. Interfaces 3, 1411–1417.
Thapliyal, P.C., Singh, K., 2014. Aerogels as Promising Thermal Insulating Materials: An Overview. J. Mater. 2014.
Ul Haq, E., Zaidi, S.F.A., Zubair, M., Abdul Karim, M.R., Padmanabhan, S.K., Licciulli, A., 2017. Hydrophobic silica aerogel glass-fibre composite with higher strength and thermal insulation based on methyltrimethoxysilane (MTMS) precursor. Energy Build. 151, 494–500. https://doi.org/10.1016/j.enbuild.2017.07.003
van Olphen, H., 1967. Polyelectrolyte reinforced aerogels of clays - Application as chromatographic absorbents. Clays Clay Miner. 15, 423–435. https://doi.org/10.1346/CCMN.1967.0150142
Wang, L., 2015. Aerogels based on biodegradable polymers and clay (PhD Thesis). Universitat Politècnica de Catalunya, Barcelona.
Wang, L., Schiraldi, D.A., Sanchez-Soto, M., 2014. Foamlike Xanthan Gum/Clay Aerogel Composites and Tailoring Properties by Blending with Agar. Ind. Eng. Chem. Res. 53, 7680–7687.
Wang, Y., Gawryla, M.D., Schiraldi, D.A., 2013. Effects of freezing conditions on the morphology and mechanical properties of clay and polymer/clay aerogels. J. Appl. Polym. Sci. 129, 1637–1641. https://doi.org/10.1002/app.39143
Zach, J., Slávik, R., Novák, V., 2016. Investigation of the Process of Heat Transfer in the Structure of Thermal Insulation Materials Based on Natural Fibres. Ecol. New Build. Mater. Prod. 2016 151, 352–359. https://doi.org/10.1016/j.proeng.2016.07.389